

Differential Cross Sections for Coherent and Incoherent Neutral-Pion Photoproduction from Calcium

G. Koch, H. Ströher,^(a) G. Breitbach, V. Metag, and S. Tschesche
II. Physikalisches Institut, Universität Giessen, D-6300 Giessen, West Germany

R. Beck, F. Kalleicher, B. Schoch, and J. Vogt
Institut für Kernphysik, Universität Mainz, D-6500 Mainz, West Germany

J. C. McGeorge, J. D. Kellie, and S. J. Hall
Kelvin Laboratory, University of Glasgow, United Kingdom
 (Received 13 February 1989)

Differential and absolute cross sections for the coherent reaction $^{40}\text{Ca}(\gamma, \pi^0)^{40}\text{Ca}_{(\text{g.s.})}$, as well as for the incoherent reaction $^{40}\text{Ca}(\gamma, \pi^0)^{40}\text{Ca}^*$ have been measured with monochromatic photons in the threshold region ($E_\gamma=157\text{--}169$ MeV). The differential cross section for the coherent process exhibits a diffraction minimum due to the nuclear mass form factor while the incoherent cross section is rather structureless. The cross sections are in good agreement with recent distorted-wave impulse-approximation calculations.

PACS numbers: 25.20.Lj

Photoproduction of neutral pions from complex nuclei is one of the most promising tools to study the production, propagation, and decay of the $\Delta(1232)$ resonance in the nuclear medium, since the elementary process ($\gamma + N \rightarrow \pi^0 + N$) is almost completely dominated by resonant production. Even near threshold resonant production prevails, in contrast to photoproduction of charged pions or elastic photon scattering which are governed by background Born terms. In addition, near the production threshold the mean free path of the produced low-energy neutral pions is expected to be larger than in the Δ -resonance region, thereby reducing the influence of final-state interactions. Studies of *near-threshold* neutral-meson production thus provide a particular clean experimental approach to investigate in-medium excitation and propagation of the Δ resonance. A quantitative comparison of accurate near-threshold measurements with conventional plane-wave impulse-approximation (PWIA) and distorted-wave impulse-approximation (DWIA) calculations will reveal the applicability of these approaches in this energy regime. Specifically, one can test the underlying assumption that dynamical modifications of the elementary operator can be neglected.

The resonant production amplitude is of particular importance for *coherent* π^0 production from even-even nuclei: In this case the nucleus is left in its ground state so that the initial and the final states of the nucleus are identical. The spin-independent part of the elementary production amplitudes of all nucleons adds up *coherently*, leading to an A^2 scaling of the cross section, which is therefore significantly enhanced compared to the cross section for charged-pion photoproduction. Besides the coherent process, neutral-pion photoproduction can also leave the nucleus in an excited state, which may either

be bound or particle unstable. These so-called *incoherent* production processes certainly exhaust a large fraction of the total cross section in the resonance region,¹ but their contribution for energies below ≈ 200 MeV has not yet been studied in detail.

Only in one experiment,¹ using an active ^{12}C target, has it been possible to discriminate between pion production leading to particle-unstable states and all other processes. In addition, for the nucleus ^4He it was possible² to separate the coherent part of the cross section, because the energies of all excited states in ^4He are large (≈ 20 MeV) compared to the pion energy resolution. These measurements have been performed near the Δ resonance and no equivalent data are available near threshold.

This Letter presents for the first time results for coherent as well as incoherent differential and total cross sections for neutral-pion photoproduction from a heavy nucleus (^{40}Ca) near threshold. The experiments have been performed at the Mainz Microtron MAMI A,³ using the Glasgow tagger⁴ in combination with the Mainz-Giessen π^0 spectrometer.⁵ A dc electron beam of 183 MeV, provided by MAMI A, was used to produce monochromatic photons by means of bremsstrahlung tagging. In the energy range 157–169 MeV chosen for the present study the energy resolution of the tagging spectrometer is ≈ 200 keV. The tagged photon flux was $1.5 \times 10^7/\text{s}$ with the π^0 spectrometer at backward angles and $0.6 \times 10^7/\text{s}$ at 0° , respectively. The flux limitation at forward angles was due to a high count rate ($\approx 10^6/\text{s}$) in the plastic scintillators in front of the lead-glass blocks of the π^0 spectrometer which were used to veto charged particles mainly from pair creation in the target. The π^0 spectrometer was placed at seven angles with respect to the photon beam direction ($0^\circ, 30^\circ, 40^\circ, 70^\circ, 90^\circ, 115^\circ,$

and 140°). Since the angular acceptance of the spectrometer is $\pm 25^\circ$ the full angular range was covered. The absolute pion detection efficiency determined in Monte Carlo simulations varies between 4% and 15% for the spectrometer settings at 90° and 0° , respectively.⁵

A target of natural calcium (96.9% ^{40}Ca) with a thickness of 8.5 g/cm^2 was used which leads to an absorption of $\approx 11\%$ of the incident photon flux. Monte Carlo calculations show that the probability for pair conversion of one of the π^0 -decay photons in the target is $\approx 30\%$ almost independent of the pion emission angle. An energy calibration of the π^0 spectrometer was performed prior to the experiment with cosmic rays. A precise energy calibration for each detector was obtained using the symmetric π^0 decay which was selected by a cut on the opening angle ($\Phi_{\gamma\gamma} \approx \Phi_{\gamma\gamma}^{\text{min}}$) for a given photon energy. The position resolution was 45 mm,⁶ achieved by the center-of-gravity method, implying an opening angle resolution of 8° . Neglecting the finite beam spot and target size the resolution would be 6.5° .

Combining energy and angular information, the pion energy and the invariant mass, as well as the pion emission angle, can be reconstructed event by event with resolutions of 9 MeV for E_{π^0} and 60 MeV for m_{inv} ,⁵ respectively. The resolution of the pion emission angle depends on the pion energy as well as the emission angle and is on the average 10° .^{6,7}

Neutral pions were identified unambiguously event by event by a cut in a two-dimensional plot of invariant mass versus opening angle. Because of the tagging technique, this sample contains random events which were subtracted using appropriate cuts in the time spectra.

Differential cross sections were obtained for photon energy bins of 2 MeV and angular bins of 4° . In Fig. 1(a) the differential cross section $d\sigma/d\Omega$ is plotted for $E_\gamma = 168 \pm 1 \text{ MeV}$ as a function of the pion emission angle in the laboratory system for *all* identified neutral pions. The angular distribution is forward peaked with a maximum at $\approx 40^\circ$ and levels off at $\approx 10 \mu\text{b/sr}$ for angles $\theta_{\pi^0} \geq 90^\circ$. The general shape of the distribution is easily understood, since due to angular momentum conservation one expects a $\sin^2\theta$ behavior for the c.m. differential cross section of coherent π^0 production on spin-zero nuclei, modified by the square of the nuclear mass form factor $F(q)$ (see Ref. 7). A diffraction minimum at around 100° due to the minimum in the form factor⁸ is, however, not observed in Fig. 1(a). As shown below, this minimum is filled in by incoherent production processes.

The contribution of incoherent π^0 production has been determined by studying the mean pion energy $\langle E_{\pi^0} \rangle$ as a function of the pion emission angle ϑ_{lab} [Fig. 1(b)]. At forward angles $\langle E_{\pi^0} \rangle$ is equal to the incident photon energy corrected for the nuclear recoil, indicating that all available energy is going to the neutral pion (i.e., coherent production). For larger emission angles $\langle E_{\pi^0} \rangle$ decreases, with a shallow minimum around 100° . The

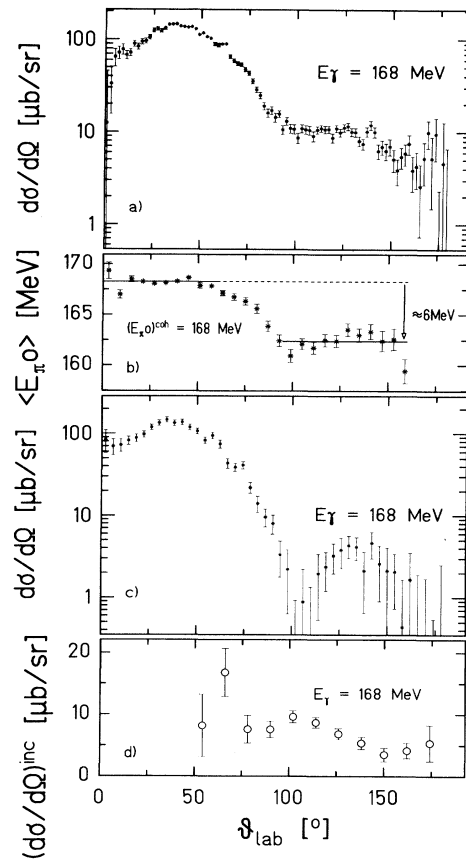


FIG. 1. Results for the reaction $^{40}\text{Ca}(\gamma, \pi^0)$ at $E_\gamma = 168 \text{ MeV}$. (a) Differential cross section for *all* neutral pions. (b) Average pion energy as a function of the emission angle. (c) Differential cross section for *coherent* pion production. (d) Differential cross section for *incoherent* pion production. The numbers given in the figure correspond to the photon beam energy in (a), (c), and (d). In (b) the number corresponds to the energy of the pion expected for coherent production $(E_{\pi^0})^{\text{coh}} = E_\gamma - E_{\text{recoil}}(\vartheta)$.

average energy shift (including also elastic events) is 6 MeV. This decrease is interpreted as arising from incoherent processes in which part of the available energy is used to excite the Ca nucleus and consequently is missing in E_{π^0} . The ratio of coherent to incoherent processes is reflected by the shift in $\langle E_{\pi^0} \rangle$. Therefore the minimum will occur where the coherent contribution is smallest which is at the diffraction minimum of the form factor. In this angular region the energy shift is 8 MeV, which is identical with the average excitation energy of the ^{40}Ca nucleus.

Because of the only moderate energy resolution of the lead-glass detectors⁵ it is not possible to discriminate between coherent and incoherent neutral-pion production event by event. However, it is possible to separate the coherent part of the cross section, using only the position information of the decay photons. For a given pion ener-

gy the opening angle $\Phi_{\gamma\gamma}$ between the two decay photons is distributed between a minimum value $\Phi_{\gamma\gamma}^{\min} = 2 \times \arcsin(m_0 c^2 / E_{\pi^0})$ and 180° with $\Phi_{\gamma\gamma}^{\min}$ being strongly favored by phase space (Jacobian peak distribution).⁹

In incoherent pion production the energy of the emitted pion is reduced by the excitation energy of the nucleus, leading to $(\Phi_{\gamma\gamma}^{\min})^{\text{incoh}} > (\Phi_{\gamma\gamma}^{\min})^{\text{coh}}$. Since for ^{40}Ca the first excited state is at 3.35 MeV; the minimum opening angle for incoherent production must be at least 4° larger than for coherent pion production. For the typical excitation energy of 8 MeV the difference in the opening angle in the coherent and incoherent reactions is 9° , compared to an opening-angle resolution of 8° . A corresponding cut on the opening-angle distribution strongly selects coherent production. Monte Carlo simulations show that for a spectrometer setting at 90° and 8° -wide cut $\Phi_{\gamma\gamma} < (\Phi_{\gamma\gamma}^{\min})^{\text{coh}}$ implies an efficiency of the spectrometer for coherent events of 5.3×10^{-3} . For incoherent events the efficiency is reduced to 1.7×10^{-3} and 4.0×10^{-5} for excitation energies in ^{40}Ca of 3.35 and 8 MeV, respectively. The absolute value of the spectrometer efficiency depends strongly on the applied cut while the variation with the pion emission angle is less than 5%. The coherent differential cross sections have thus been normalized with respect to the differential cross sections for all produced pions assuming only coherent pion production in the angular range $\theta_{\pi^0} = 20^\circ - 50^\circ$. This separation between coherent and incoherent events can be applied in the threshold region studied here, where the opening angle depends strongly on the pion energy.

After applying this analysis a diffractive study already observed in elastic electron scattering data is seen for the first time in the differential cross section for coherent photoproduction of neutral pions [Fig. 1(c)]. The momentum transfer covered in this energy range is $0.3 - 1.4 \text{ fm}^{-1}$. Consequently, only one minimum appears at $\approx 100^\circ$. For the other investigated energies it shifts as expected to $\approx 110^\circ$ at $E_\gamma = 160 \text{ MeV}$.

The difference between Figs. 1(a) and 1(c) is attributed to the incoherent cross section. For small angles the subtraction of two large but nearly identical cross sections results in large statistical errors, but the results become significant for angles greater than 75° [Fig. 1(d)]. The differential cross section is rather structureless, as is to be expected if a large number of excited states with different form factors are involved.

In Fig. 2 the angle-integrated differential cross sections for *all* events as well as for coherent and incoherent π^0 production are plotted as a function of the incident photon energy. σ_{all} and σ_{coh} have been obtained from an angular integration of the corresponding differential cross section. The incoherent cross section [Fig. 2(b)] has been integrated at backward angles ($\vartheta = 90^\circ - 180^\circ$). All cross sections rise rapidly with increasing photon energy. The increase is stronger for incoherent production, reflecting the exponentially increasing number of possi-

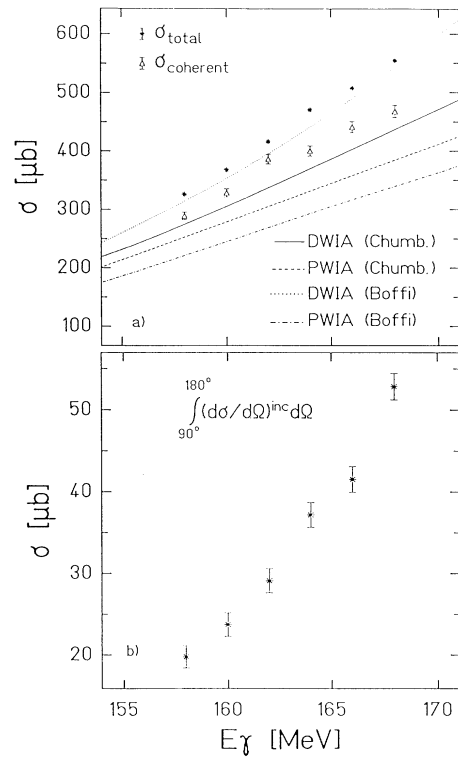


FIG. 2. Integrated cross sections as a function of the photon beam energy. (a) For *all* and *coherently produced* pions compared with the calculations of Refs. 10 and 11. (b) Integrated ($90^\circ - 180^\circ$) *incoherent* cross section.

ble final states.

Figure 3 shows a comparison of our results with calculations of Kamalov¹² and Chumbalov *et al.*¹⁰ in the impulse approximation. The calculations have been folded with the angular resolution of our π^0 spectrometer. The

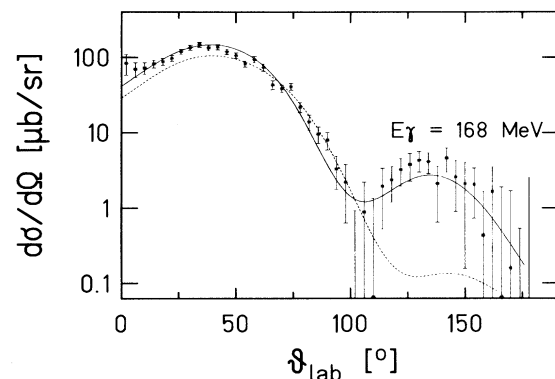


FIG. 3. Differential *coherent* cross section for the reaction $^{40}\text{Ca}(\gamma, \pi^0)$. Comparison with PWIA (dotted line) and DWIA calculations (solid line) of Refs. 10 and 12. Both calculations have been folded with the experimental angular resolution, which varies between 7° (at 90°) and 14° (at 0°).

calculation neglecting final-state interactions (PWIA) fails to reproduce the measured cross sections, in particular the position of the diffraction minimum and the yield in the second maximum. Final-state interactions are taken into account by DWIA calculations, which reproduce the data much better, especially at backward angles. The attractive πN potential modifies the outgoing pion momentum thereby increasing the effective momentum transfer. This in turn leads to a shift of the diffraction minimum and to a larger increase of the cross section at backward angles via the nuclear form factor. Extraction of a root-mean-square mass radius¹³ can only be performed reliably with a detailed knowledge of the final-state interaction.

The DWIA and PWIA calculations are based on the elementary production operator as treated in Ref. 14. It should be pointed out, however, that this elementary operator leads to multipoles¹⁵ which are *not* in agreement with the experimentally determined values for π^0 production from the nucleon.^{16,17} This subject will be treated in a forthcoming paper. Unfortunately, calculations in the Δ -hole model are not yet available for the energies considered here.

In summary, we have performed a measurement of the (γ, π^0) reaction on ^{40}Ca near threshold. It has been possible to divide the total (differential and angle integrated) cross sections into coherent and incoherent contributions. The coherent cross section exhibits a minimum due to the nuclear mass form factor, which could be used to obtain information on the nuclear mass distribution provided the final-state interaction is known precisely. A comparison with PWIA and DWIA calculations indicates the importance of including final-state interactions. Calculations within the Δ -hole model may shed more light on the role of the Δ excitation in the production of neutral pions and their propagation in the nuclear medium. For future experiments in the Δ -resonance region a high-resolution spectrometer for neutral-meson detection

is under construction.¹⁸

We would like to thank K. H. Kaiser and the operator staff of the MAMI A accelerator for providing the excellent and stable electron beams. We are grateful to Ch. Berger (Rheinisch-Westfälische Technische Hochschule Aachen) for providing the lead-glass detectors. This work was supported in part by Deutsche Forschungsgemeinschaft Sonderforschungsbereich 201.

(a)Now at Gesellschaft für Schwerionenforschung, Darmstadt, West Germany.

¹J. Arends *et al.*, *Z. Phys. A* **311**, 367 (1983).

²D. R. Tieger *et al.*, *Phys. Rev. Lett.* **53**, 755 (1984).

³H. Herminghaus *et al.*, *Nucl. Instrum. Methods* **138**, 1 (1976).

⁴J. D. Kellie *et al.*, *Nucl. Instrum. Methods Phys. Res., Sect. A* **241**, 153 (1985).

⁵H. Ströher *et al.*, *Nucl. Instrum. Methods Phys. Res., Sect. A* **269**, 568 (1988).

⁶G. Koch, Ph.D. thesis, University of Giessen, 1988 (unpublished).

⁷G. Koch *et al.*, *Phys. Lett. B* **218**, 143 (1989).

⁸C. W. DeJager *et al.*, *At. Data Nucl. Data Tables* **14**, 479 (1974).

⁹G. Källen, *Elementary Particle Physics* (Addison-Wesley, Reading, MA, 1964).

¹⁰A. A. Chumbalov *et al.*, *Z. Phys. A* **328**, 195 (1987).

¹¹S. Boffi and R. Mirando, *Nucl. Phys. A* **448**, 637 (1986).

¹²S. S. Kamalov (private communication).

¹³R. A. Schrack *et al.*, *Phys. Rev.* **127**, 1772 (1962).

¹⁴I. Blomqvist and J. M. Laget, *Nucl. Phys. A* **280**, 405 (1977).

¹⁵A. A. Chumbalov *et al.*, *Phys. Lett. B* **213**, 255 (1988).

¹⁶E. Mazzucato *et al.*, *Phys. Rev. Lett.* **57**, 3144 (1986).

¹⁷R. Beck, Ph.D. thesis, University of Mainz, 1989 (unpublished).

¹⁸V. Metag and R. S. Simon, Gesellschaft für Schwerionenforschung Darmstadt Report No. 87-19 (to be published).